Research Article GU J Sci, Part A, 9(4): 461-473 (2022) https://doi.org/10.54287/gujsa.1189756

Gazi University
Journal of Science
PART A: ENGINEERING AND INNOVATION
http://dergipark.org.tr/gujsa

# Characterization of Hot Extruded Hybrid Composites Al 2024 Metal Matrix Reinforced with $TiO_2$ and $ZrO_2$

Ayşenur PEKTAŞ[1,2*] Okan Can EBETÜRK[3] Uğur GÖKMEN[3]

[1]*Gazi University, Institute of Science and Technology, Department of Advanced Technologies, Ankara, Türkiye*
[2]*KTO Karatay University, School of Applied Sciences, Department of Flight Training, Konya, Türkiye*
[3]*Gazi University, Institute of Science and Technology, Department of Metallurgical and Materials Engineering, Ankara, Türkiye*

**Keywords**

Hybrid Composites
Powder Metallurgy
Hot Press Method
Radiation Shielding

**Abstract**

In this study, the microstructure and mechanical properties of Al 2024 powder, the prominent type of Al 2XXX series aluminum alloys widely used in the aerospace industry, and $TiO_2$ and $ZrO_2$ reinforcement elements used to improve material properties were investigated. Each reinforcement element is included in the material at the rate of 10%. For hybrid composite sample production, 10% hybrid composite material was procured by adding each reinforcing element equally. For each sample, powders were mixed in a 3D mixer to ensure an equal distribution of matrix powder and reinforcement elements in the samples. The samples were churned out by subjecting the two-stage them to a one-way hot press process. The furnace temperature was kept at 600 °C to preserve samples. Density and microstructure analyses were performed on the formed samples, and the results were evaluated. After all, the Archimedean density measurement method was used to obtain final densities, these samples were taken to bakelite for optical images, then scanning electron microscope (SEM) and Brinell hardness of the samples was measured. The cross-fracture strength test was completed to analyze each sample's microstructural behavior. Finally, the theoretical radiation shielding properties of each sample were investigated. The Phy-X/PSD program was used to examine the radiation permeability properties. According to the test and analysis results, the effect of reinforcement elements on the material was determined. As a result, the highest hardness value measured was 97.5 HB at the 10% $ZrO_2$ -reinforced MMCs. However, the relative density of the hybrid composite is better than $ZrO_2$-reinforced MMCs. Thus, the best cross-fracture strength measured was 635 MPa in 10% hybrid MMCs. The radiation shielding parameters showed that the 10% $ZrO_2$ -reinforced MMCs are best for shielding. Therefore, the second reasonable material for radiation shielding is hybrid reinforced materials. In the final decision, hybrid composite materials became prominent because the distinctive features of each material enhanced the samples.

**Cite**

Pektaş, A., Ebetürk, O., &Gökmen, U. (2022). Characterization of Hot Extruded Hybrid Composites Al 2024 Matrix Reinforced with $TiO_2$ and $ZrO_2$. *GU J Sci, Part A, 9*(4), 461-473.

**Author ID (ORCID Number)**

A. Pektaş, 0000-0002-9448-1591
O. C. Ebetürk, 0000-0002-5324-6018
U. Gökmen, 0000-0002-6903-0297

**Article Process**

**Submission Date** 15.10.2022
**Revision Date** 24.10.2022
**Accepted Date** 09.11.2022
**Published Date** 31.12.2022

## 1. INTRODUCTION

Composites, which are widely used in aviation, are preferred in the industry because they improve the physical and mechanical properties of the structure. However, composites reinforced with various reinforcing elements, such as ceramics, have become the materials sought in the aerospace industry by providing good wear resistance, high hardness, strength, and improvements in corrosion resistance (Naito et al., 2021). The widely preferred aluminum matrix composites combine critical lightness and high-strength properties. Features such as high wear, low density, and flexible production ability play an essential role in the aerospace industry's preference for aluminum matrix composites (Naito et al., 2021). 2XXX series aluminum alloys are distinguished from other series due to their superior machinability and are frequently preferred in aircraft structures and the automotive industry. $ZrO_2$ and $TiO_2$ materials have higher densities, according to aluminum compounds. Though, they are used as reinforcement elements in MMCs, they improve the properties of

*Corresponding Author, e-mail: ayse.nur.pektas@karatay.edu.tr

materials. The zirconia particles are expected to increase the strength and toughness of the composite due to their ability to undergo the stress-induced transformation from a tetragonal to a monoclinic phase (Eckner et al., 2016). Titanium dioxide has properties like chemical stability, good optical transparency, wear resistance, and mechanical and good thermal properties (Joshua et al., 2018).

This research examines the mechanical properties of Al 2024 metal matrix composites enriched with $TiO_2$ and $ZrO_2$ reinforcing elements to evaluate their use in aerospace. $TiO_2$ and $ZrO_2$ can be examples of ceramic materials added to the aluminum matrix to form composite materials. At the same time, hybrid composites containing $TiO_2$ and $ZrO_2$ ceramic particles offer better properties by taking advantage of the mechanical properties of two different reinforcement elements. Composite material production can be achieved in different ways. In this study, three different metal matrix composite samples were produced using the powder metallurgy method. The powder metallurgy method provides distinct advantages, such as homogeneous reinforcing element distribution and reasonable microstructure control (Gökmen, 2016; Alekhya, 2022). The samples produced as 10% $TiO_2$, 10% $ZrO_2$, and 10% hybrid by weight were produced by powder metallurgy method at Gazi University laboratories and formed by applying the hot-pressing method. After the hot-pressing method, the effect of reinforcement ratio on the microstructure and mechanical properties of the composite material was determined by obtaining optical images, scanning electron microscope, cross-fracture tests, and radiation permeability analysis.

Most known and common radiation shielding materials are generally lead-based and polymeric structures (McAlister, 2018). $TiO_2$ is a good choice because it is a chemically stable material, and it is known for its mechanical properties to improve the flexural and compressive strength of the composite (Nikbin et al., 2019; Park et al., 2019). The $ZrO_2$ envelopes the $TiO_2$ with its decent hardness value to become a suitable shielding material. As far as is known, there is no available data about the radiation shielding properties of $TiO_2$ and $ZrO_2$-based aluminum matrix hybrid composites. Hence, this study enlightens the microstructural properties of selected materials and investigates radiation shielding parameters to widen the literature.

## 2. MATERIAL AND METHOD

### 2.1. Material

In this research, metal matrix composite samples were produced by Powder Metallurgy (PM) and hot-pressing methods. The matrix material is pre-alloyed Al 2024, and $TiO_2$ and $ZrO_2$ powders are used as reinforcement elements. The powder's SEM images do not exist. Though, the SEM images are taken after the production of each sample. The matrix alloy's chemical composition and the powders' physical properties are given in Table 1 and 2, respectively.

***Table 1.*** *Chemical Composition of the Matrix Alloy*

| **Element** | **Cu** | **Mn** | **Mg** | **Fe** | **Al** |
|---|---|---|---|---|---|
| **Rate (Weight %)** | 4,4 | 1,8 | 0,25 | 0,5 | Other |

***Table 2.*** *Physical Properties of Powders Used*

| **Material** | **Physical Properties** | | |
|---|---|---|---|
| | Density (g/cm$^3$) | Melting Temperature (°C) | Powder Size (μm) |
| **Al 2024** | 2,74 | 502-638 | 20 μm |
| **$TiO_2$** | 4,26 | 1843 | 1 μm |
| **$ZrO_2$** | 5,68 | 2370 | 20 μm |

### 2.2. Method

Pre-alloyed Al 2024 powder was mixed separately in a three-dimensional mixer as separate samples, containing 10% $TiO_2$ and 10% $ZrO_2$ by weight. Afterward, 10% hybrid composite powder was mixed in which 5% $TiO_2$ and 5% $ZrO_2$ were included simultaneously. The turbulent mixer was run for 30 minutes for each sample to homogenize. Next, the mixed powders were exposed to a pressure of 400 MPa on a one-way press machine and sintered for 1 hour by being thrown into the vacuumed furnace at 600 ℃. At the end of the period, the mold removed from the furnace was again subjected to 800 MPa pressure on a one-way pressure machine, and then the sample was left to cool. The sample dimensions obtained are 31.2*12.6*6.35 mm. After the cooling process, the samples removed from the mold were cut by wire erosion to become cross-fracture test products by powder metal sample standards (MPFI-41, 1998).

In the present study, three metal matrix composite samples containing 10% reinforcement elements were obtained using a hot press with the PM method. Three samples were produced from each reinforcement material matrix composite, and nine samples were used in the experiments. For sample production, each reinforcement element and Al 2024 were added to the mixing bowl in the determined proportions and mixed with a turbular mixer for 30 minutes until they became homogeneous. The powder mixtures obtained were taken into the lubricated mold and first pressed with a uniaxial hydraulic press under a load of 10 tons and made compact. After pressing, the samples were kept in the oven at 600 ℃ for 1 hour and pressed again under 20 tons of load. Materials whose sample production was completed were subjected to a 3-point bending test. Then, bakelite was taken from the broken samples to obtain optical images, and the surface roughness was removed. After all, the SEM images were obtained. The gamma behaviors of a novel shielding material of Al 2024 Metal Matrix Reinforced with $TiO_2$ and $ZrO_2$ were also investigated. The shielding effectiveness of these materials for gamma-ray has not been studied until now. In this work, for the first time, the LAC, MAC, TVL, HVL, and MFP of Al 2024 Metal Matrix Reinforced with $TiO_2$ and $ZrO_2$ using the Phy-X platform were theoretically calculated considering the radiation shielding. Furthermore, all the values calculated for these composite materials by running the Phy-X platform were compared.

### 2.3. Characterization

Densities of the samples produced by applying a hot press with powder metallurgy method were determined according to Archimedes principle by using Sartorius brand balance with 0.0001 g precision and density kit. The composite samples obtained were sanded under water with 240-400-800-1200 grit sandpapers for characterization and then polished using 1 and 3 μm diamond paste on the polishing felts. The interfaces of $ZrO_2$ and $TiO_2$ particles dispersed in the produced hybrid composites with the matrix material were examined with the help of a Leica brand optical microscope and JEOL JSM 6060LV Scanning Electron Microscope (SEM), and EDS analyzes were made. Fractured surfaces were characterized with the help of SEM. The hardness measurements of the composite samples were measured as Brinell using the Emco test duravision 2000 brand hardness measuring device. The hardness values were determined by taking the average measurements from 5 regions for each sample. Cross-fracture tests of sintered and extruded samples were performed using Instron 3369 model test device. Cross-fracture tests were performed by taking the average of 3 samples for each composite. MPIF Standard 41 and previous studies were taken as references in preparing the test samples and executing the tests (Gökmen, 2016).

## 3. RESULTS AND DISCUSSION

### 3.1. Density and Microstructure Analysis

The densities are calculated for manufactured composites, and the microstructure of the samples is characterized. As the density of Al 2024 is 2.78 g/cm$^3$, the reinforcement materials, which are $TiO_2$'s density is 4.26 g/cm$^3$, and $ZrO_2$'s density is 5.68 g/cm$^3$. Thus, the content ratio of each sample is 10% mixed with 90% Al 2024. In the beginning, theoretical densities are calculated, as shown below.

$$d_{10\%\,TiO_2} = \frac{90\%\,(Al2024) + 10\%\,(TiO_2)}{100} \qquad d_{10\%\,TiO_2} = \frac{250.2 + 42.6}{100} = 2.928\frac{g}{cm^3}$$

$$d_{10\%\,ZrO_2} = \frac{90\%\,(Al2024) + 10\%\,(ZrO_2)}{100} \qquad d_{10\%\,ZrO_2} = \frac{250.2 + 56.8}{100} = 3.07\frac{g}{cm^3}$$

$$d_{10\%\,Hybrid} = \frac{90\%\,(Al2024) + 5\%\,(TiO_2) + 5\%\,(ZrO_2)}{100} \qquad d_{10\%\,Hybrid} = \frac{250.2 + 28.4 + 21.3}{100} = 2.998\frac{g}{cm^3}$$

The theoretical density of 10% $TiO_2$ reinforced Al 2024 is 2.93 g/cm$^3$, 10% $ZrO_2$ reinforced Al 2024 is 3.07 g/cm$^3$, and finally, the 10% hybrid (5% both $TiO_2$ and $ZrO_2$) reinforced Al 2024 metal matrix composite is calculated as 2.99 g/cm$^3$. After the sample production, the density of each sample is calculated according to the principles of Archimedes. In Figure 1, the comparison of the theoretical and actual densities is graphed. The Archimedes density results are lower than the theoretical densities of the samples. The closer results are obtained in Al 2024 without reinforcement element, and the most distant results are observed in 10% $ZrO_2$ reinforced MMCs. In the metal matrix composite prepared by using both reinforcement elements, changes in the density values were determined after the sintering and pressing processes. Even if the reinforcement element percentage is the same for every sample, we are getting different densities because the particle size used is different for each element powder. It is known that as the particle size increases, the powder metal material's density will decrease (Rahimian et al., 2009).

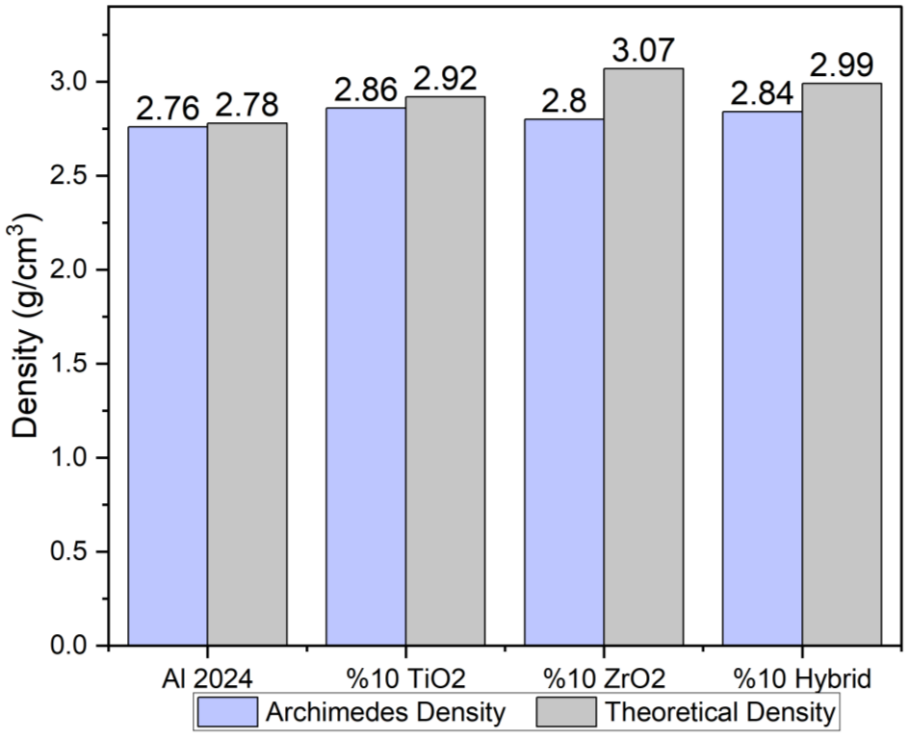


***Figure 1.*** *Comparison between the theoretical and the Archimedes density for each sample*

Figure 2 shows the optical microscope images of 10% $TiO_2$, 10% $ZrO_2$, and 10% Hybrid composite samples. Figure 2 includes the maximized microstructural images showing the relation between the particle and matrix material interface. It is observed that particles are dispersed equally in the Al 2024 matrix with the guidance of these figures. Also, the micropores are independent of each other and when these images are analyzed there are partial flocculation occurs in material samples.

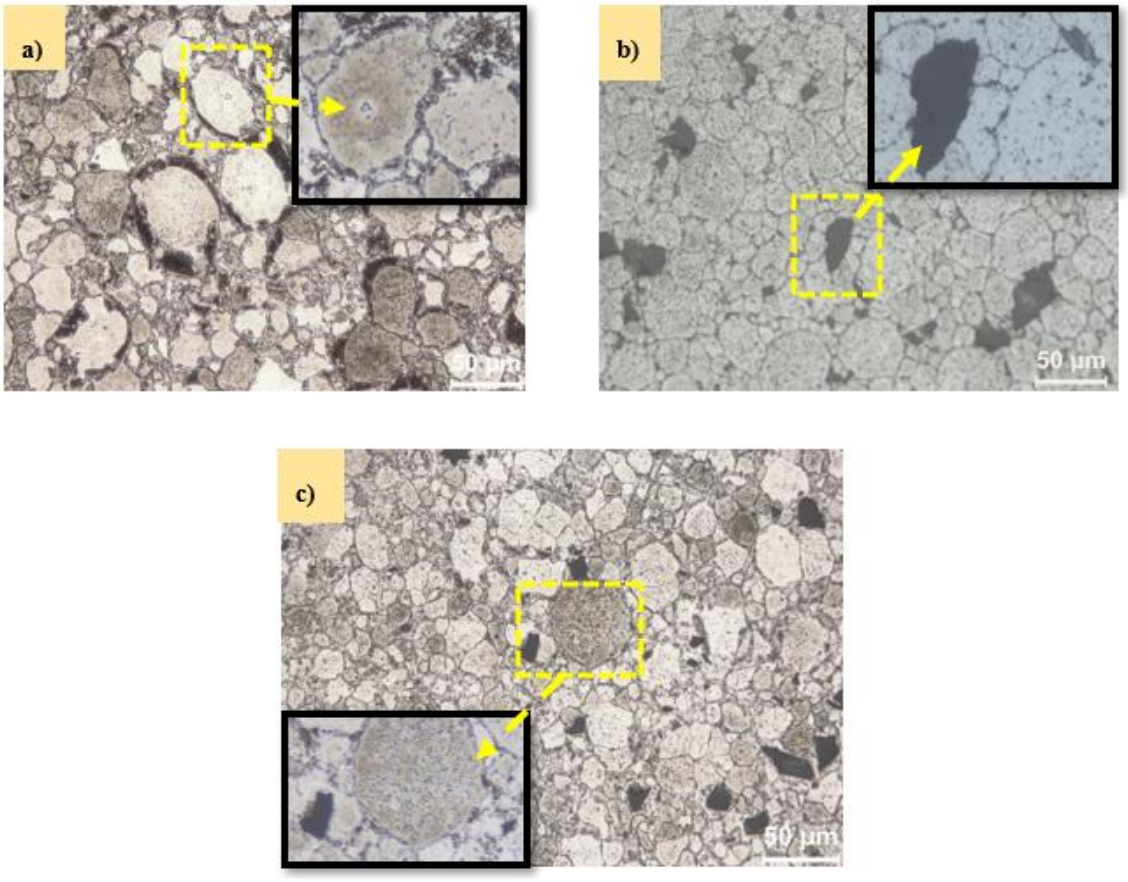


***Figure 2. a)*** *Optical image of 10% $TiO_2$ reinforced Al 2024,* ***b)*** *Optical image of 10% $ZrO_2$ reinforced Al 2024,* ***c)*** *Optical image of 10% Hybrid reinforced Al 2024*

After the optical microscope images are taken, the EDS analysis is done to analyze the elemental distribution of each sample.

Figure 3 and 4 show the selected point's elemental distribution of $TiO_2$ and $ZrO_2$ separately. At point number 2 for Figure 3a, it can be seen that $TiO_2$ and Al 2024 materials are mixed, and the intermediate phase is comprised. For Figure 3b and 4b, The $ZrO_2$ is clearly observed in point 1.

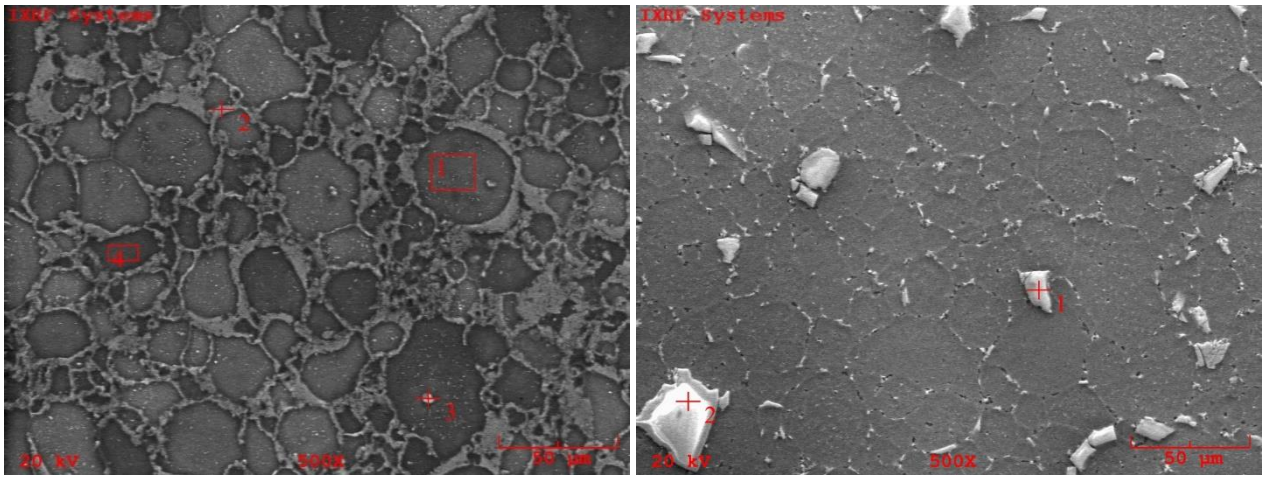


***Figure 3. a)*** *EDS image of 10% $TiO_2$ reinforced Al 2024,* ***b)*** *EDS image of 10% $ZrO_2$ reinforced Al 2024*

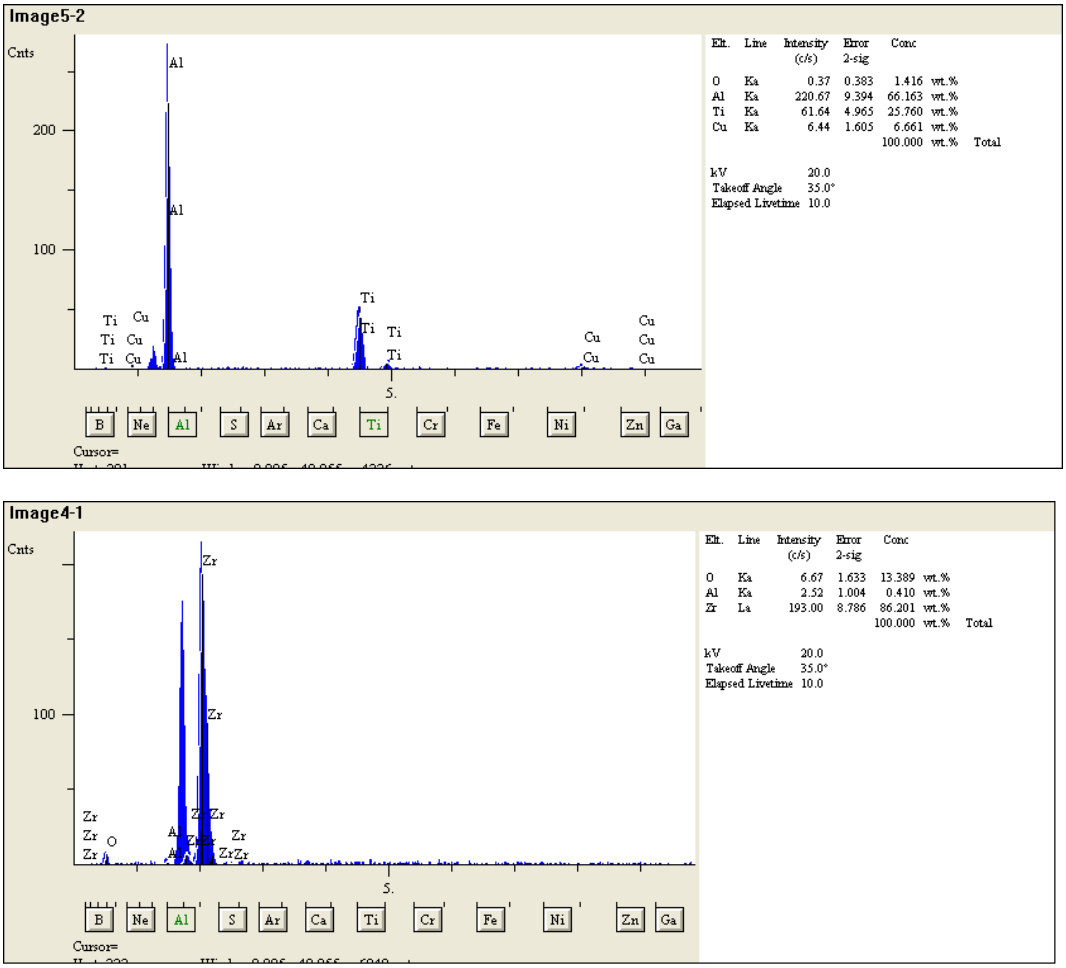


***Figure 4. a)*** *Elemental analysis for obtained points in 10% $TiO_2$ reinforced Al 2024 image,* ***b)*** *Elemental analysis for obtained points in 10% $ZrO_2$ reinforced Al 2024 image*

The hybrid composite sample's EDS analysis resulted in Figures 5 and 6. The obtained points 2 and 4 are investigated in figures. As a result, the $ZrO_2$, $TiO_2$, and the compounds of Al 2024 were observed from EDS analysis.

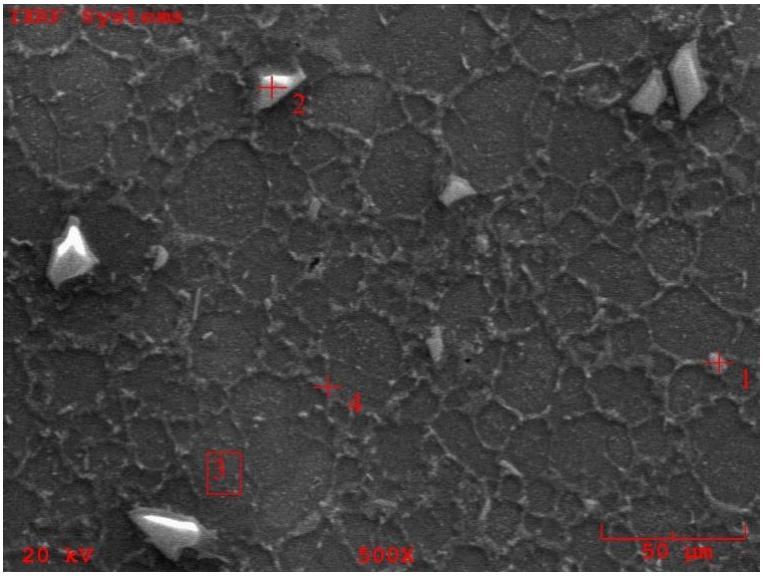


***Figure 5.*** *EDS image of 10% hybrid reinforced Al 2024*

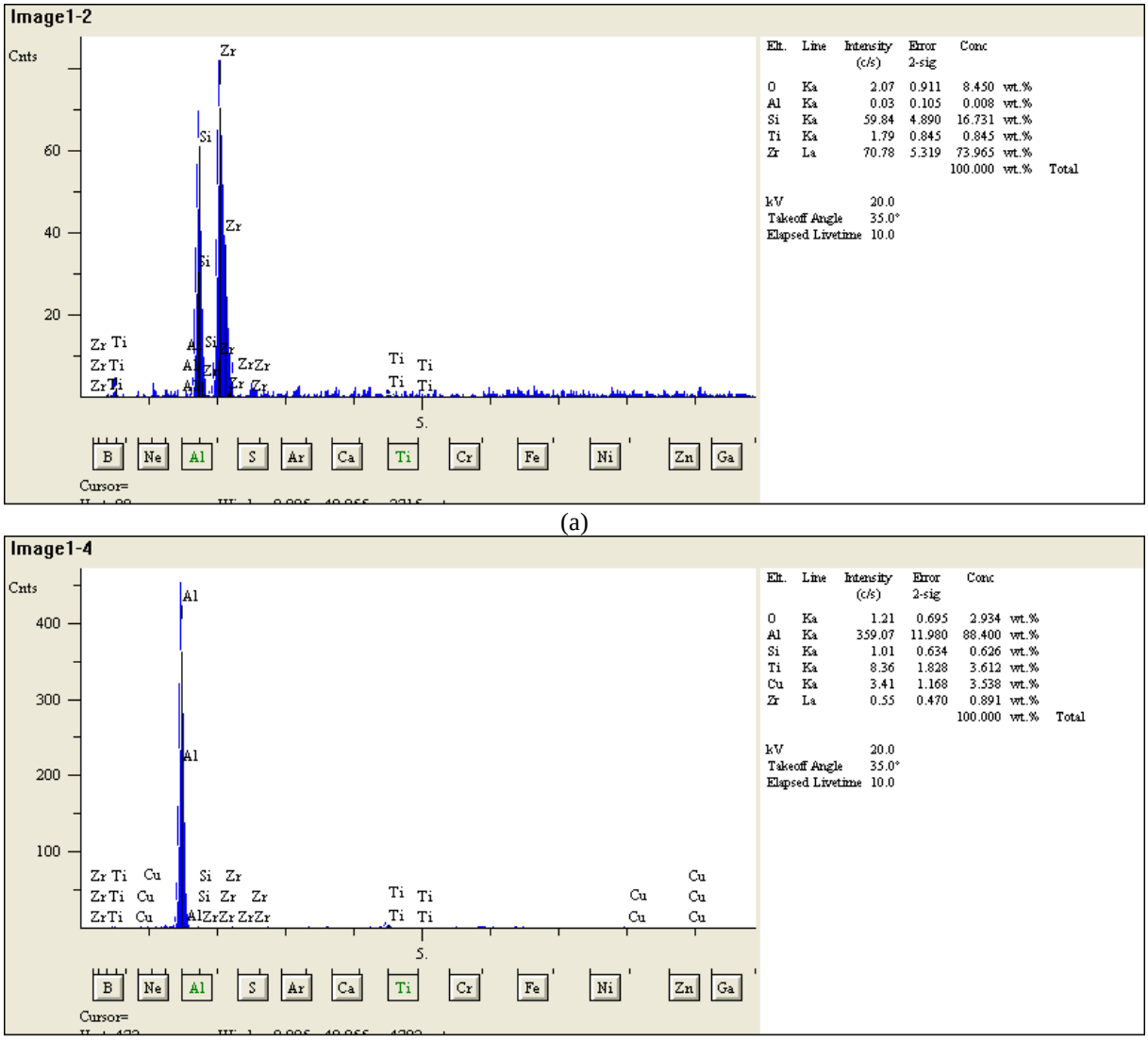


***Figure 6. a)*** *Elemental analysis for point 2 in 10% hybrid reinforced Al 2024 image,* ***b)*** *Elemental analysis for point 4 in 10% hybrid reinforced Al 2024 image*

The SEM images after the hot press given in Figure 7 supports the partial aggregation detected between the Al 2024 matrix and the particles. It is known that in powdered metal composite materials, particles cause agglomeration and pores, and this affects the material's performance (Dobrzański et al., 2005). In the examinations, it was observed that the agglomeration caused by the reinforcement particles in the structure before the extrusion process occurred more, the agglomerations were distributed after the extrusion process, and a more homogeneous structure was formed.

SEM images showing the distribution of $TiO_2$ and $ZrO_2$ particles in the Al 2024 matrix are given in Figure 3. According to the images given in Figure 3, it can be said that the particles existing in the composite are homogeneously distributed. Partial voids were observed between the matrix surface and $TiO_2$ and $ZrO_2$ particles, as well as partial particle aggregation in some regions according to the SEM images given in Figure 7, at 7b and 7c. However, it has been determined that these particle aggregations do not exist in the entire composite structure. It is thought that the hot extrusion process disperses the particle aggregations and supports the homogeneity of the ceramic particle distribution in the matrix. Gaps were observed between the Al 2024 matrix and the ceramic particles. When the SEM image of the hybrid composite given in Figure 7, at 7d is examined, it is seen that the $ZrO_2$ particles are partially clustered around the $TiO_2$ particles.

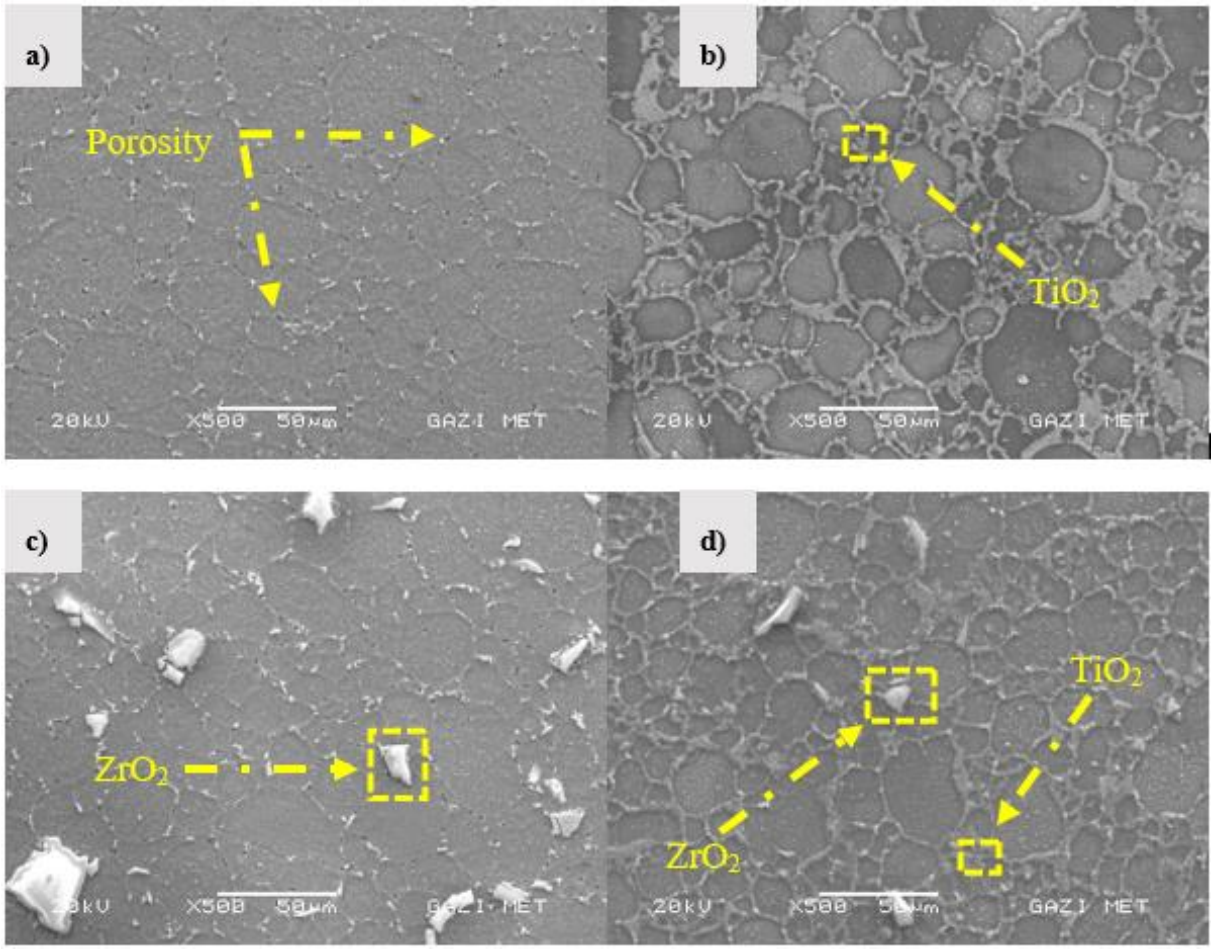


***Figure 7. a)*** *SEM image of Al 2024,* ***b)*** *SEM image of 10% $TiO_2$ reinforced Al 2024,* ***c)*** *SEM image of 10% $ZrO_2$ reinforced Al 2024,* ***d)*** *SEM image of 10% Hybrid reinforced Al 2024*

### 3.2. Mechanical Properties

In Figure 8, each $TiO_2$ and $ZrO_2$ reinforced Al 2024 hot-pressed metal matrix composite's Brinell hardness values can be reviewed. It is normal to observe that as the particle amount increases in the Al 2024 matrix, the hardness increases (Leyi et al., 2011). The lowest hardness value is measured at 80.52 HB in 10% TiO2-reinforced Al 2024 elements. Also, the highest hardness value is observed in 10% ZrO2-reinforced Al 2024 material. That makes sense to get a hybrid metal matrix composite's hardness is 83.74 HB, an average for overall observation. The highest hardness value is measured as 97.5 HB in the Al 2024 sample containing 10% by weight of $ZrO_2$. When the hardness values of samples containing the same amount of $TiO_2$ and $ZrO_2$ in the Al 2024 matrix are compared, it is observed that the hardness values of the composites containing $ZrO_2$ are significantly higher.

In the literature, it is known that $ZrO_2$ particles have higher hardness values according to the $TiO_2$ particle (Kumar et al., 2019; Paul & Islam, 2021). It was determined that the hardness value of the Al 2024 matrix with the $TiO_2$ and $ZrO_2$ reinforced hybrid composite was higher than the composite sample containing 10% $TiO_2$reinforced Al 2024 matrix composite. It is thought that the 5% $ZrO_2$, which is one-half of the 10% reinforcement elements in the hybrid composite, together with the high density obtained after the pressing process caused an increase in hardness value.

In Figure 9, the strength and elongation values obtained after the cross-fracture test applied to Al 2024 MMCs are given. Ceramic-based composites have high hardness values, and they need to be produced in smaller dimensions. Thus, the TRS method is optimum for ceramic-based MMCs. Tensile stress is the most common and one of the most accurate tests to measure the elastic deformation of the sample. Nevertheless, this research focused on the effect of porosity ratios on the sample's rupture strength. Porosity is an important problem in

parts produced with powder metallurgy. This test method is interesting because the transverse rupture strength test is very sensitive to porosity levels (Fang, 2005). The highest cross-fracture strength was obtained in the composite sample reinforced with 10% Hybrid with 635 MPa. The cross-fracture value obtained in the composite samples containing $ZrO_2$ was higher than the samples reinforced with $TiO_2$. The highest elongation amount reached in the produced MMCs was determined in Al 2024 samples without reinforcement elements, and the lowest elongation value was determined in composites containing 10% $TiO_2$. The change observed in the elongation values is parallel with the hardness of the MMCs. It is thought that the change observed in the cross fracture and elongation amounts of 10% hybrid composite materials is due to the increase in density in parallel with this situation, where the $TiO_2$ and $ZrO_2$ particles gather around each other and improve the particle/matrix interface with the extrusion process. The cross-fracture strength relates to the hardness values of the material. It is expected that materials with high hardness also have high cross-fracture strength (Kim et al., 2005; Qian et al., 2005). Thus, the materials containing $ZrO_2$ particles showed better cross-fracture strength than the $TiO_2$-reinforced MMCs in Figure 9. The hybrid composite sample has the best strength because the relative density results of the hybrid composite are better than the $ZrO_2$-reinforced MMCs. As the relative density increases, the porosity amount decreases. In addition to this, the material's strength against dislocation formation increases (Bin et al., 2006; Kim et al., 2016). Figure 9 shows that the hybrid MMC sample resulted from better cross-fracture strength than the $ZrO_2$-reinforced MMCs.

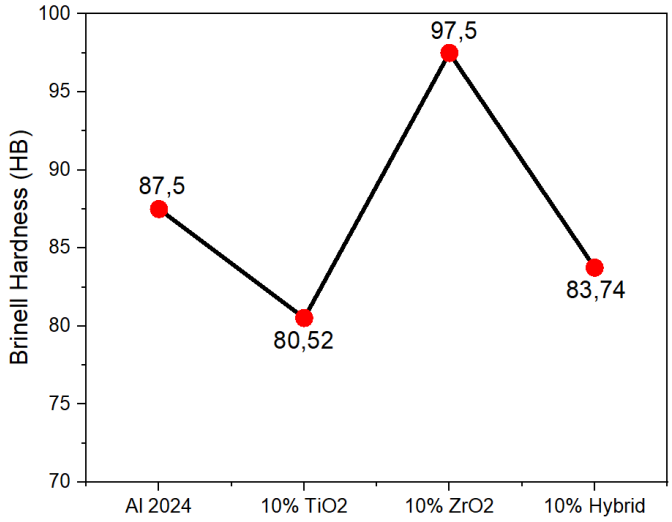


***Figure 8.*** *Brinnel Hardness Test Results of Samples*

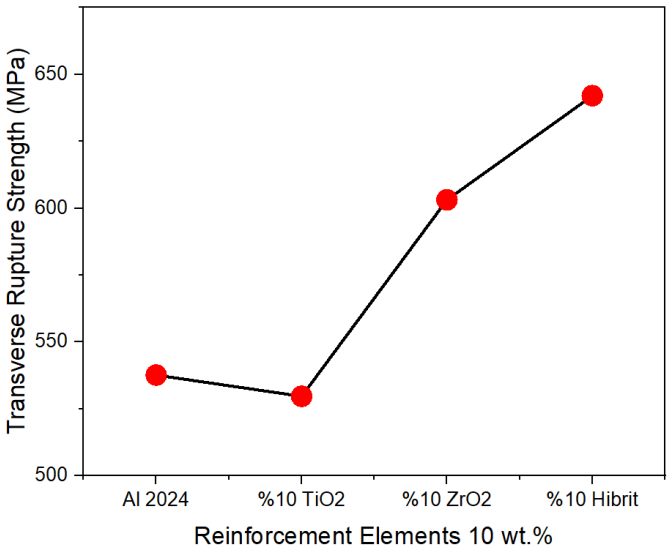


***Figure 9.*** *Transverse Rupture Strength Results of 10 wt. % Reinforcement Elements with Al 2024*

### 3.3. Radiation Shielding

Radiation can be defined as the energy traveling in the medium. The source of radiation can be investigated as natural and artificial. (Gökmen et al., 2022) Natural radiation sources are radiation that occurs without human contribution. Also, the radiation can be examined in two subtopics which are ionizing and non-ionizing radiation. The alpha, beta, and neutron particles are particle-based ionizing radiations, and the X and gamma rays are electromagnetic radiations (Sürücü & Subaşı, 2021; Gökmen et al., 2022). The situation that distinguishes ionizing radiation from non-ionizing radiation is that the charge balance in the atom is disrupted as a result of ionizing radiation removing electrons from the atom or binding electrons to the atom (Sürücü & Subaşı, 2021).

As seen in Figure 10a, the lowest LAC value among the samples was calculated as Al 2024 without reinforcement. The LAC values of the other samples are pretty close to each other. However, when evaluated among them, the highest LAC value was measured as 10% doped $ZrO_2$. The samples following this value are hybrid-doped Al 2024 and 10% doped $TiO_2$, respectively. The LAC value generally decreases and increases inversely with the energy. The MAC value is procured by dividing the LAC values by the sample densities. Accordingly, Figure 10b shows that the lowest MAC value was calculated for Al 2024 without reinforcement material, while the highest MAC value was assessed as 10% doped $TiO_2$. In general, HVL and TVL values were examined in Figure 11 to determine the material that gives the best shielding properties among the four composite materials. The material thickness values required for material radiation shielding increased in direct proportion to the increase in energy. The sample Al 2024 without reinforcement that required the most material thickness for shielding was approximately 10 cm for HVL, while it was 40 cm for TVL. The half-value layer of the 10% $ZrO_2$ reinforced MMCs are measured at ~9 cm, and the tenth-value layer is measured at ~32 cm. The material requiring the lowest thickness was determined as 10% doped $ZrO_2$. In this case, the best shielding properties were determined as 10% doped $ZrO_2$, 10% doped hybrid, 10% doped $TiO_2$, and undoped Al 2024, respectively. Figure 12 shows that the distance required for photon collision is less in low-energy regions, but the distance increases gradually in higher energy ranges where pair production and Compton scattering can occur. The lowest distance is measured at ~13 cm in 10% $ZrO_2$-reinforced MMCs. Figure 13 shows the effective atomic mass number and the number of electrons of each sample. Results showed that 10% $ZrO_2$-reinforced MMCs are significantly higher than others.

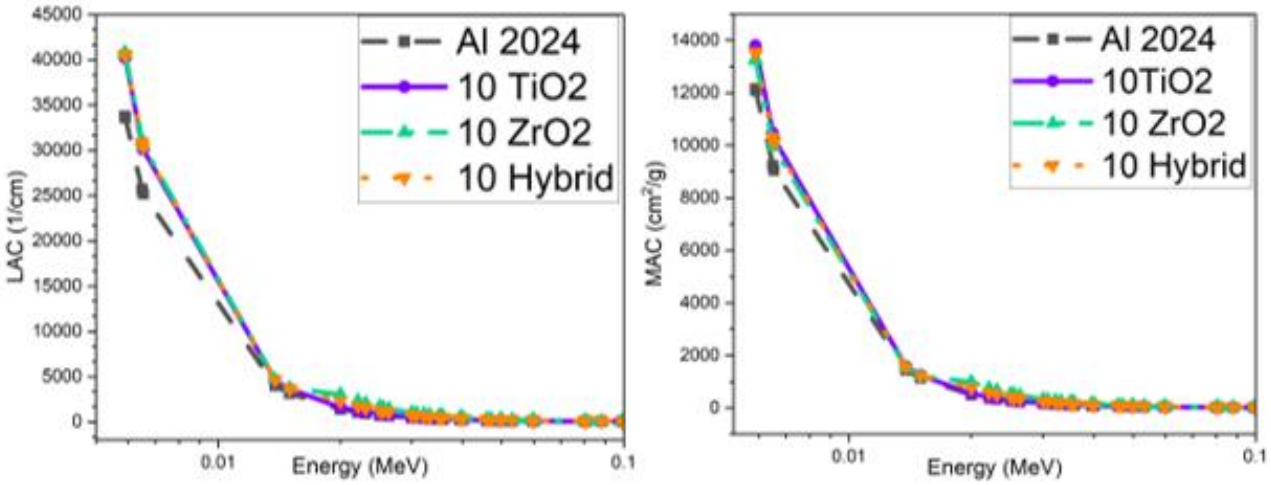


***Figure 10. a)*** *The linear attenuation coefficient of each sample versus Energy,* ***b)*** *The mass attenuation coefficient of each sample versus Energy*

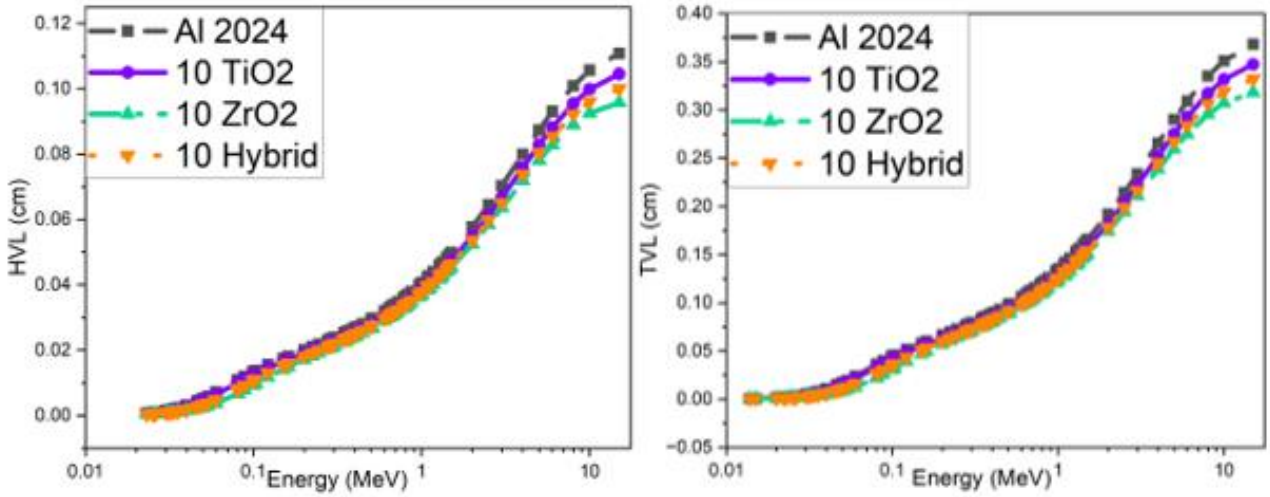


***Figure 11. a)*** *The half-value layer alteration of each sample versus Energy,* ***b)*** *The tenth-value layer alteration of each sample versus Energy*

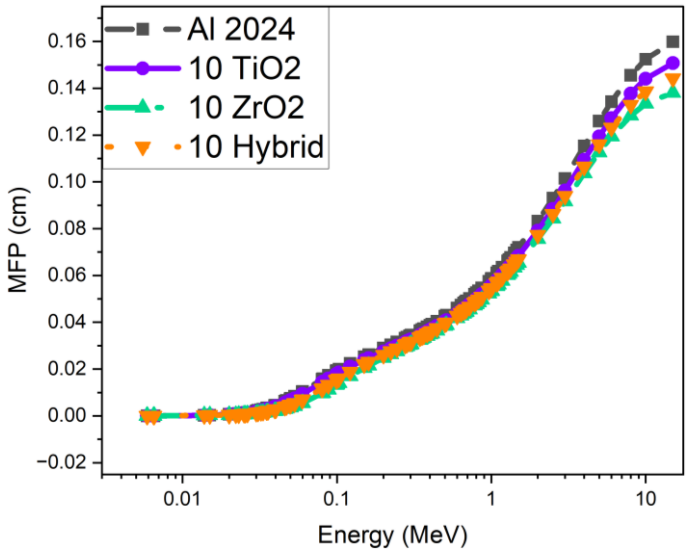


***Figure 12.*** *The mean free path alteration of each sample versus Energy*

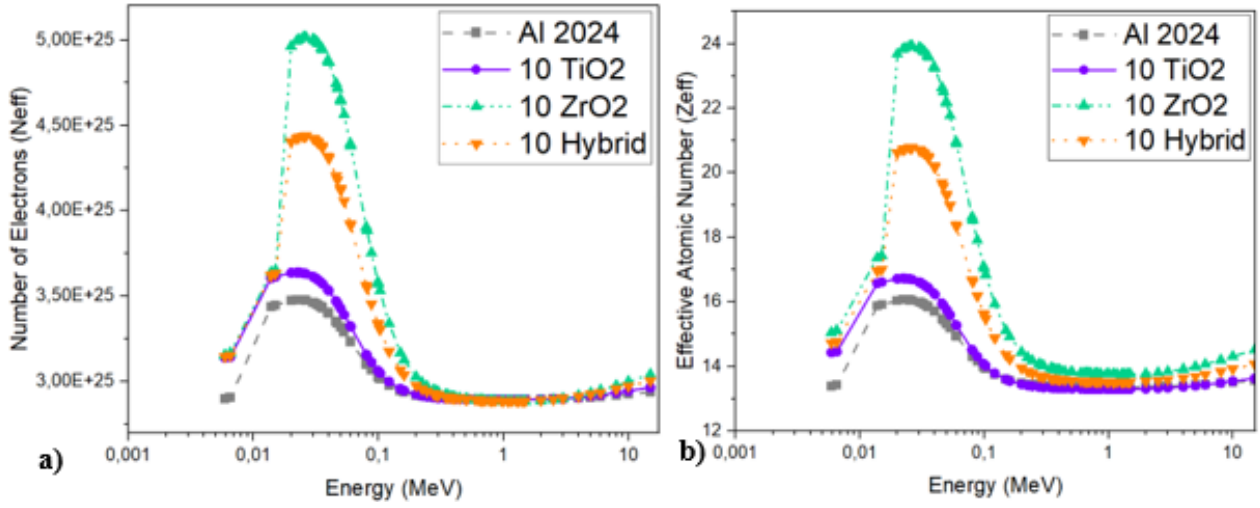


***Figure 13. a)*** *The effective atomic mass number alteration of each sample versus Energy,* ***b)*** *The number of electrons of each sample versus Energy*

## 4. CONCLUSION

The samples are produced by the powder metallurgy method. For each sample, the production method, which is a hot-pressed powder metallurgy method, is done to strengthen the samples. After all, optical images of these samples are taken from bakelite. The optical images show that the materials mixed homogeneously and the porosity distribution over the sample. The highest hardness value among the samples taken from Brinell hardness values was observed as 97.5 HB in 10% ZrO2-added samples. After that, a 3-point bending test was done to investigate the relationship between the maximum load applied to the sample and the elastic deformation. The TRS test was the best option due to the sample size. Results show that the maximum load is read in a 10% hybrid reinforced Al 2024 sample. The maximum applied load at the breaking point is calculated as 9180.713 N. The maximum flexural stress at break is also read in the 10% Hybrid reinforced Al 2024 sample. In conclusion, the Radiation shielding test results, the MAC, LAC, HVL, TVL, and MFP values are calculated. When the radiation shielding values of the samples are examined, LAC and MAC values show the absorption capacity of the material. High values indicate a good absorption capacity. The HVL, TVL, and MFP values determine the shielding properties. Low values indicate that the material has a good shielding capacity. According to the logarithmic increase in energy, the most absorptive sample is observed as a 10% $ZrO_2$-reinforced Al 2024 sample. The hybrid composite sample has close results with the 10% $ZrO_2$. The most vulnerable material from all of the samples is decided as Al 2024 sample without reinforcement. This leads us to understand that each material and reinforcement element have different advantages, and they provide improvement for the material's shielding properties.

## ACKNOWLEDGEMENT

The author expresses his gratitude to Gazi University Scientific Research Projects Office (Project No: FGA-2022-7521) for the financial support.

## CONFLICT OF INTEREST

The authors declare no conflict of interest.

## REFERENCES

Alekhya, Ch., Prajoshna, A., Baig, M. A., Chandrika, Ch., Devaraju, A., & Gadakary, S. (2022). Preperation and characterization of Al-$TiO_2$-Mg composites through powder metallurgy. *Materials Today: Proceedings*, *66*(2), 489-495. doi:10.1016/j.matpr.2022.03.725

Bin, J., Zejun, W., & Naiqin, Z. (2006). Effect of pore size and relative density on the mechanical properties of open cell aluminum foams. *Scripta Materialia*, *56*(2), 169-172. doi:10.1016/j.scriptamat.2006.08.070

Dobrzański, L. A., Wlodarczyk, A., & Adamiak, M. (2005). Structure, properties and corrosion resistance of PM composite materials based on EN AW-2124 aluminum alloy reinforced with the $Al_2O_3$ ceramic particles. *Journal of Materials Processing Technology*, *162-163*, 27-32. doi:10.1016/j.jmatprotec.2005.02.006

Eckner, R., Krampf, M., Segel, C., & Krüger, L. (2016). Strength and fracture behaviour of a particle-reinforced transformation-thoughened trip steel/ZrO2 composite. *Mechanics of Composite Materials*, *51*(6), 707-720. doi:10.1007/s11029-016-9541-z

Fang, Z. Z. (2005). Correlation of transverse rupture strength of WC-Co with hardness. *International Journal of Refractory Metals & Hard Materials*, *23*(2), 119-127. doi:10.1016/j.ijrmhm.2004.11.005

Gökmen, U. (2016). Sıcak Ekstrüze Edilmiş Al 2024 Matrisli B4C/Al2O3 Takviyeli Hibrit Kompozitlerin Üretimi ve Karakterizasyonu. *Journal of Polytechnic*, *19*(4), 445-453.

Gökmen, U., Özkan, Z., Taşçı, U., & Ocak, S. B. (2022) Investigation of radiation shielding by adding $Al_2O_3$ and $SiO_2$ into the high-speed steel composites: comparative study. *Physica Scripta*, *97*(5), 055307. doi:10.1088/1402-4896/ac65be

Joshua, K. J., Vijay, S. J., & Selvaraj, D. P. (2018). Effects of Nano TiO2 particles on microhardness and microstructural behaviour of AA7068 metal matrix composites. *Ceramics International*, *44*(17), 20774-20781. doi:10.1016/j.ceramint.2018.08.077

Kim, C. K., Kim, Y. C., Park, J. I., Lee, S., Kim, N. J., & Yang, J. S. (2005). Effects of alloying elements on microstructure, hardness, and fracture toughness of centrifugally cast high-speed steel rolls. *Metallugical and Materials Transactioans A, 36*, 87-97. doi:10.1007/s11661-005-0141-0

Kim, Y., Jo, H., Allen, J. L., Choe, H., Wolfenstine, J., & Sakamoto, J. (2016). The effect of relative density on the mechanical properties of hot pressed cubic $Li_7La_3Zr_2O_{12}$. *Journal of the American Ceramic Society*, *99*(4), 1367-1374. doi:10.1111/jace.14084

Kumar, G. B. V., Pramod, R., Sekhar, Ch. G., Kumar, G. P., & Bhanumurthy, T. (2019). Investigation of physical, mechanical and tribological properties of Al6061–ZrO2 nano-composites. *Heliyon*, *5*(11), 02858. doi:10.1016/j.heliyon.2019.e02858

Leyi, G., Wei, Z., Jing, Z., & Songling, H. (2011). Mechanics analysis and simulation of material Brinell hardness measurement. *Measurement*, *44*(10), 2129-2137. doi:10.1016/j.measurement.2011.07.024

McAlister, D. R. (2018). *Gamma Ray Attenuation Properties of Common Shielding Materials.* PG Research Foundation, Inc. 1955 University Lane Lisle, IL 60532. PDF

Naito, M., Kitamura, H., Koike, M., Kusano, H., Kusumoto, T., Uchihori, Y., Endo, T., Hagiwara, Y., Kiyono, N., Kodama, H., Matsuo, S., Mikoshiba, R., Takami, Y., Yamanaka, M., Akiyama, H., Nishimura, W., & Kodaira, S. (2021). Applicability of composite materials for space radiation shielding of spacecraft. *Life Sciences in Space Research*, *31*(1), 71-79. doi:10.1016/j.lssr.2021.08.004

Nikbin, I. M., Mohebbi, R., Dezhampanah, S., Mehdipour, S., Mohammadi, R., & Nejat, T. (2019). Gamma ray shielding properties of heavy-weight concrete containning Nano-$TiO_2$. *Radiation Physics and Chemistry*, *162*, 157-167. doi:10.1016/j.radphyschem.2019.05.008

Park, J., Suh, H., Woo, S. M., Jeong, K., Seok, S., & Bae, S. (2019). Assesment of neutron shielding performance of nano-TiO2-incorporated cement paste by Monte Carlo simulation. *Progress in Nuclear Energy*, *117*, 103043. doi:10.1016/j.pnucene.2019.103043

Paul, S., & Islam, M. M. (2021, December 12-14). *Fabrication of Aluminum Metal Matrix Composites Reinforced with $TiO_2$ by Powder Metallurgy Techniques*. Proceedings of the International Conference on Mechanical Engineering and Renewable Energy (ICMERE 2021), Chattogram, Bangladesh.

Qian, J., Daemen, L. L., & Zhao, Y. (2005). Hardness and fracture toughness of moissanite. *Diamond and Related Materials*, *14*(10), 1669-1672. doi:10.1016/j.diamond.2005.06.007

Rahimian, M., Ehsani, N., Parvin, N., & Baharvandi, H. R. (2009). The effect of particle size, sintering temperature and sintering time on the properties of Al–$Al_2O_3$ composites, made by powder metallurgy. *Journal of Materials Processing Technology*. *209*(14), 5387-5393. doi:10.1016/j.jmatprotec.2009.04.007

Sürücü, A. M., & Subaşı, S. (2021). Nanomateryallerin Kompozit Malzemelerin Radyasyon Zırhlama Özelliklerine Etkisinin İncelenmesi. *El-Cezeri*, *8*(1), 182-194 . doi:10.31202/ecjse.812372